<u>Seminar Presentation Summary</u>

Designing Optically Tracked Instruments for Image-Guided Surgery
J.B. West, C.R. Maurer, IEEE Transactions in Med. Imaging, 2004, 23(5)

<u>Project description</u>
Virtual rigid body (VRB) brings a fresh perspective into image-guided surgical environment by detecting with stereocamera system the "virtual" light pattern projected on a surface to track surgical instruments. While its excellence is anticipated in spatially constrained circumstances as in laparoscopy, its performance has not been thoroughly evaluated. In this light, the current paper on accuracy of optical tracking is reviewed.

<u>Problem</u>
Optical tracking system consists largely of fiducial markers attached to some instrument, and optical position sensor (OPS) that measures their positions. The tracking accuracy is important in image-guided surgery to correctly determine the instrument tip position in the preoperative or intraoperative images for surgical operations. The paper aims to develop an analytic theory and experimentally evaluate the effect of the fiducial configuration, including the number of fiducials and their spatial distribution, on the tracking error of instrument tip position.

<u>Key Results</u>
1. Theory predicts that tooltip tracking error is proportional to error that OPS makes in detecting the fiducials, inversely proportional to square root of number of fiducials, and dependent on relative position of the tooltip to the fiducials.
2. Theory predicts that errors accumulate in quadrature manner with multiple registrations.
3. The tracking error of an instrument's tip position decreases as fiducials are placed closer to the instrument tip and distributed farther from each other along the axis of the tool.
4. Theoretical prediction and experimental results reflect considerable correlation.

<u>Significance</u>
- Strong correlation between the theoretical and experimental assessments of tooltip error grants convenient means to approximate the accuracy of specific configuration of fiducials from simple parameters such as their number, distance from the instrument tip, and distances between each other, which provide the basic guideline for fiducial design.

<u>Necessary background</u>
- Registration transformation
  o Point-based transformation between N points of $\{x_i\}$ and N points of $\{y_i\}$ aims to find rotation matrix R and translation vector t such that the following distance is minimized.

$$d^2 = \frac{1}{N}\sum_{i=1}^{N}|y - (Rx + t)|^2$$

o For CIS1, quaternion implementation was used.

Theory Development on Prediction of Registration Error

1. Types of errors associated with the registration and optical tracking

f : fiducial position
p : tip position
T : transformation

T_{ip}

f_i

{i}

{p}

f_p

p_i

p_p

{p} : OPS coordinate   [] : Actual
{i} : instrument coordinate   []* : Measured
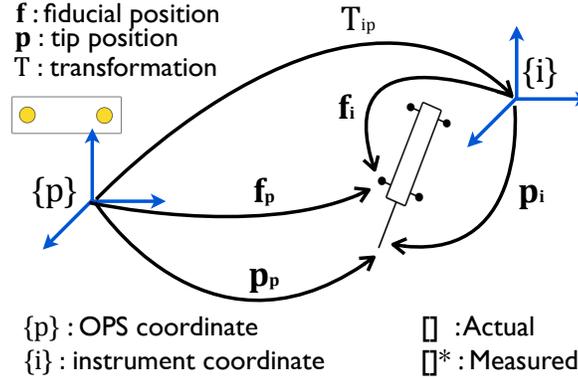
Figure 1

1) *Fiducial Localization Error* (FLE): Distance between true and measured position. For <u>each</u> fiducial j,
$$FLE_j \equiv \left\| \boldsymbol{f_{pj}^*} - \boldsymbol{f_{pj}} \right\|$$
The root-mean-square (rms) value is denoted without subscript.
$$FLE \equiv rms[FLE_1, \cdots, FLE_N] = \sqrt{\langle FLE^2 \rangle}$$
$$\text{where } \langle \cdot \rangle \equiv Expeted\ value$$

2) *Fiducial Registration Error* (FRE): Distance between the measured fiducial positions in OPS coordinate and actual fiducial in instrument coordinate mapped to the OPS coordinate.
For <u>each</u> fiducial j,
$$FRE_j \equiv \left\| \boldsymbol{f_{pj}^*} - \boldsymbol{f_{pj}} \right\| = \left\| T_{ip}^* \cdot \boldsymbol{f_{ij}^*} - T_{ip} \cdot \boldsymbol{f_{ij}^*} \right\| = \left\| T_{ip}^* \cdot \boldsymbol{f_{ij}^*} - \boldsymbol{f_{pj}} \right\|$$
The root-mean-square (rms) value is denoted without subscript.
$$FRE \equiv rms[FRE_1, \cdots, FRE_N] = \sqrt{\langle FRE^2 \rangle}$$

3) *Target Registration Error* (TRE): Distance between the measured tooltip position in OPS coordinate and actual tooltip position in instrument coordinate mapped to the OPS coordinate.
For the instrument tip,
$$TRE \equiv \left\| \boldsymbol{p_p^*} - \boldsymbol{p_p} \right\| = \left\| T_{ip}^* \cdot \boldsymbol{p_i^*} - T_{ip} \cdot \boldsymbol{p_i^*} \right\| = \left\| T_{ip}^* \cdot \boldsymbol{p_i^*} - \boldsymbol{p_p} \right\|$$

2. Statistically expected values of the point-to-point registration errors
For *N* fiducials and given tip position of the instrument $\boldsymbol{r}$
$$\langle FLE^2 \rangle = 3\sigma^2$$
$$\text{where } \sigma^2 : \text{variance of noise}$$
$$\langle FRE^2 \rangle = \frac{N-2}{N} \langle FLE^2 \rangle$$

$$\langle TRE^2(\boldsymbol{r}) \rangle = \frac{\langle FLE^2 \rangle}{N} \left(1 + \frac{1}{3} \sum_{k=1}^{3} \frac{d_k^2}{f_k^2} \right)$$

1: translational component, $\frac{1}{3}\sum_{k=1}^{3} \frac{d_k^2}{f_k^2}$: rotational component

where d_k: distance of tip position $\boldsymbol{r}$ from kth principle axis of fiducials
f_k: distance rms distance of fiducials from kth axis.

3. Application to composition of transformation

The study further develops the theory for the composition of two transformations. Specifically, in addition to OPS and surgical tool, often another set of fiducials is attached to the patients and a coordinate reference frame (CRF) is defined. CRF allows tracking the tool with respect to the patient, and freedom of moving the patient or the OPS. Such scheme is described in the figure below.

f : instrument fiducial position
p : instrument tip position
c : CRF fiducial position

{p} : OPS coordinate
{i} : instrument coordinate
{c} : CRF coordinate
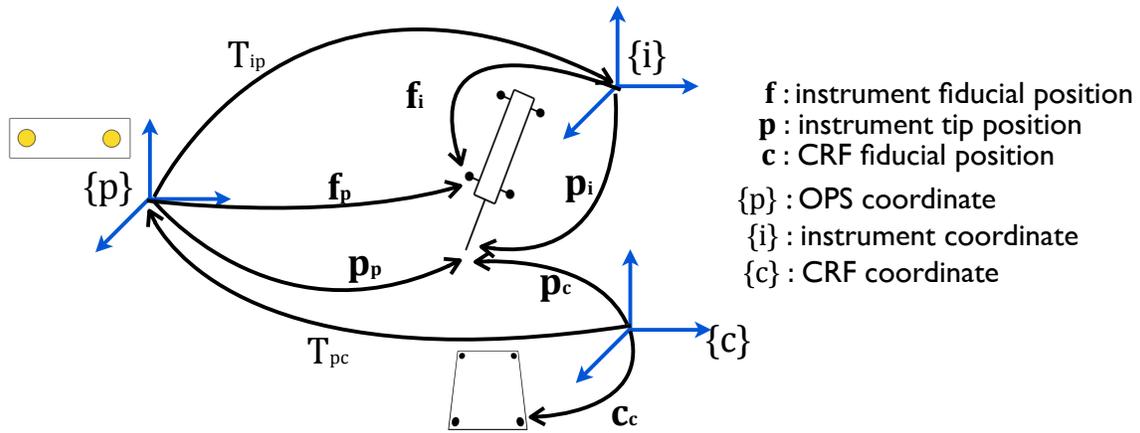
Figure 2

The model of the instrument and CRF is assumed to be perfect. $\mathbf{f_i}$, $\mathbf{p_i}$, and $\mathbf{c_c}$ are errorless and known. The instrument tip in the CRF coordinates is described by composition of transformations, $\boldsymbol{p_c} = T_{pc} \cdot T_{ip} \cdot \boldsymbol{p_i}$. Therefore, $TRE_{ip,pc}(\boldsymbol{p_c})$ includes the error from both of the registrations, T_{ip} and T_{pc}. It turns out that TRE of composition is quadrature sum of TRE of each individual transformation. The spatial map is provided in Figure 3.

$$\langle TRE_{ip,pc}^2(\boldsymbol{p_c}) \rangle = \langle TRE_{ip}^2(\boldsymbol{p_p}) \rangle + \langle TRE_{pc}^2(\boldsymbol{p_c}) \rangle$$

$$\langle TRE_{ip,pc}^2(\boldsymbol{p_c}) \rangle \quad = \quad \langle TRE_{ip}^2(\boldsymbol{p_p}) \rangle \quad + \quad \langle TRE_{pc}^2(\boldsymbol{p_c}) \rangle$$
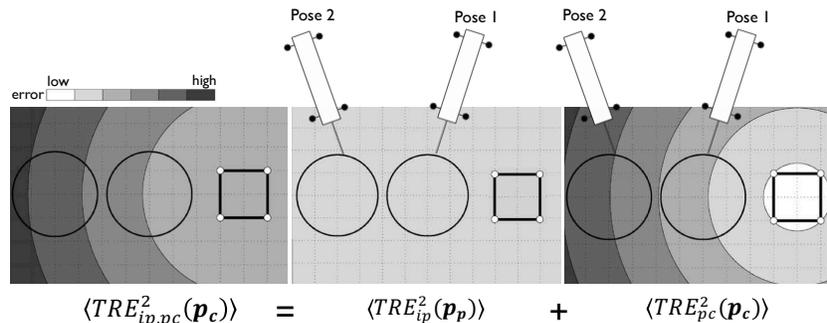
Figure 3

Simulation on Registration Error Prediction

A numerical simulation of composition $\langle TRE^2_{ip,pc}(\boldsymbol{p_c})\rangle$ was performed in the following steps, and its scheme is illustrated in Figure 2. A given vector or transformation with an asterisk (*) signifies that it is actual, and without an asterisk signifies it is measured.

1. Choose arbitrary actual, "known" values: $\boldsymbol{c_c^*}, \boldsymbol{f_i^*}, T_{ic}^*, T_{cp}^*$
2. Compute actual values $\boldsymbol{p_c^*}, \boldsymbol{f_c^*}, \boldsymbol{c_p^*}, \boldsymbol{p_p^*}, \boldsymbol{f_p^*}$
3. Simulate OPS measurements $\boldsymbol{c_p}, \boldsymbol{p_p}$, by adding noise with $\sigma = \frac{FLE}{\sqrt{3}}$, where FLE values are provided by the manufacturer of the OPS.
4. Compute transformations T_{pc}, T_{ip} from measured values
5. The actual and measured values pointer tool in CRF: $\boldsymbol{p_c^*} = T_{ic}^*(\boldsymbol{p_i^*}), \boldsymbol{p_c} = T_{pc} \cdot T_{ip}(\boldsymbol{p_i^*})$
6. $\langle TRE^2_{ip,pc}(\boldsymbol{p_c})\rangle = \|\boldsymbol{p_c} - \boldsymbol{p_c^*}\|^2$
7. Loop 1-6 100000 times, and calculate rms value of the acquired TREs.
8. Perform simulation at various locations with respective to CRF.

Experiment on Registration Error Prediction

1. Setup

Ground truth of a 4 x 4 grid of "divots" spaced at 20mm is manufactured, and CRF is rigidly attached level to the divot grid. Parameter r denotes the distance of CRF fiducials from the centroid of CRF, and d denotes the distance from the divot grid center to centroid of CRF. The used instrument and its fiducials are illustrated on the right of Figure 4 below, as well as the setup on the left. Parameters A, B and ρ define the distribution of fiducials. Tooltip position of the instrument is obtained by pivot calibration using more than 1000 measurements.
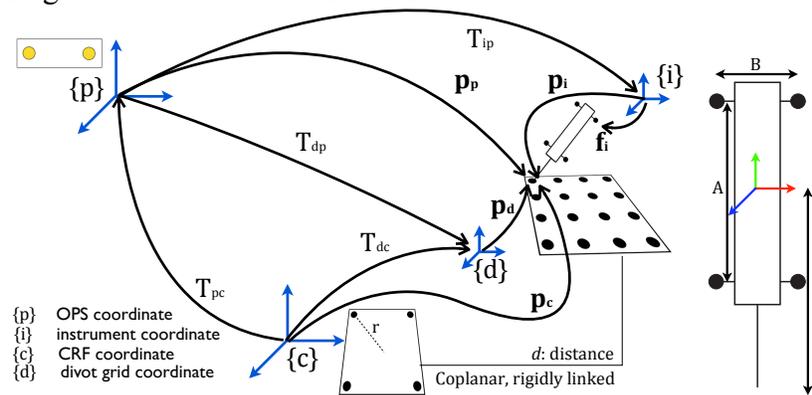
Figure 4

2. FRE measurement and TRE calculation

FRE is obtained by placing the probe in each of 16 divots, recording each measured tip position in OPS coordinate, registering to the divot grid, and calculating the registration error. From FRE, TRE is calculated using the developed prediction model.

$$TRE_m = \sqrt{\frac{N}{N-2}} FRE$$

3. Experimental combinations
- Fiducial distribution

2 types of ρ, 2 types of r, and 4 types of d
- Position/Orientation of instrument, divot grid, CRF
   A. Orientation of the tool at each divot is constant, and the positions of divots grid and CRF are fixed.
   B. Orientation of the tool at each divot is random, and the positions of divots grid and CRF are fixed.
   C. Orientation of the tool, and positions of divot grid and CRF are random.
      Note: Measurements are static.
- Three Types of OPS/fiducial marker
      Optotrack 3020 / Active, Polaris / Active, Polaris /Passive

Results
Results showed considerable match with theoretical prediction, with correlation coefficient of 0.82 and slope of linear regression of 0.97.

Assessment
The study was an excellent survey of registration problem in optical tracking, encompassing the fundamental concepts, development of a theory, its validation by comparison with simulations and experiments, and suggestion of general guidelines for designing optical fiducial markers. Furthermore, such topics were discussed not only in generic perspective but also in the context of registration between OPS, surgical instrument and CRF, giving insights for application in the actual surgical environment. That the theoretical prediction and experimental results were coherent – higher accuracy with smaller fiducal distance from tooltip and larger distance from each other – provides convenient and reliable means for designing such markers. This supports the proposed advantage of VRB in applications such as laparoscopy. First, conventional rigid bodies are most likely attached to the backmost part of the laparoscope, or farthest from the tip of the laparoscope. On the other hand, virtual rigid bodies, projected on the surface of the patient body, are much closer to the tooltip. Second, it is much easier to spread out the fiducial markers in the virtual rigid bodies. These two factors point towards enhanced accuracy using virtual rigid bodies.

Another useful aspect of the study was classification of different types of registration errors, which must all be considered in comparison between physical and virtual rigid bodies. As discussed above, while spatial distribution of VRB anticipates higher *registration* accuracy, its *localization* accuracy must also be considered, since VRB requires detection of some pattern of projected light, which may be different from detection of physical markers. For now, we control the effect of detection system's performance on localization accuracy, by using the same detection hardware and software, MicronTracker, for both types of rigid bodies. The difference inherent in the two types of rigid bodies will still need to be kept in mind.

A little insufficient was the experimental evaluation of instrument fiducial distribution. For example, lengths A and B between fiducials were unaltered. Also, the effect of fiducials' *rotational* distribution on the tracking accuracy would have been useful. The experiments investigated the different *translational* distances between the fiducials. The

effect of angular differences between fiducials is also of interest, since in virtual rigid body, the projected fiducial markers become considerably skewed when the tool, and the attached projector, is slanted. The issue also applies to the distance between the fiducials and the tooltip. While the differential linear distance (ρ) is studied, the angular differences are not included in the study, which again can be very useful for accuracy assessment of VRB. Similarly, the study focuses on translational target registration error. The rotational TRE would also be of great interest, and the study does mention it in the very last part of discussion section. Further works on this issue are expected.

More quantitative analysis of the experimental results on effect of fiducial configuration on tracking error may have been insightful. The study generally states that the trend fits with the theoretical model. It would be great to know in detail how certain parameters fit better, and discuss some factors behind discrepancies.

Finally, the study would be more helpful with experimental evaluation of fully passive markers, as those in MicronTracker.